

SIMULATION AND EVALUATION OF SLIDING MODE CONTROLLER FOR ELBOW EXOSKELETON SYSTEMS

Huthaifa Al-Khazraji^{1*}, Aws M. Abdullah², Hussien Dulaimi³

^{1,3}University of Technology-Iraq, Baghdad, Iraq

²University of Baghdad, Baghdad, Iraq

Emails: ^{1*}60141@uotechnology.edu.iq, ²aws.abd@cois.uobaghdad.edu.iq, ³60179@uotechnology.edu.iq

Abstract - Joint dysfunction disables are impacting millions of individuals worldwide. It significantly interferes with essential daily tasks like eating, drinking, and writing, often making self-care challenging for those affected. Exoskeleton robots are developed to enable individuals with impaired physical functions to perform daily activities and maintain independence. This study introduces a wearable exoskeleton control system for the elbow joint designed, providing an alternative assistive solution to traditional treatment methods. The elbow exoskeleton system used for therapy has nonlinearity and time-dependent parameters. To address these challenges, this work presents a sliding mode control (SMC) for tracking the path of an EES. To reduce the chattering phenomenon in the SMC, power rate (PR) and boundary layer (BL) reaching laws are introduced. The heap-based algorithm (HBA) is used to tune design parameters of SMC. Massive simulations that were implemented in MATLAB confirmed the effectiveness of the suggested methodologies as they proved the reduction in the chattering and the improvement in the system performance. The simulation outcomes reveal that both approaches are able to eliminate the chattering phenomenon. However, the value of the IAE of the system controlled by SMC with the PR reaching law is reduced by 42.7% in compares with the system controlled by SMC with the BL reaching law. In addition, the IAE under uncertainty has been improved by 43.9%.

Keywords: Elbow rehabilitation, Nonlinear control system, Sliding mode control, Power rate reaching law, Boundary layer reaching law, Heap-based algorithm.

1. Introduction

Each year, many people experience disability as a result of joint dysfunction caused by various factors such as aging and/or stroke. For example, every year, approximately 13.7 million new incidents of stroke are reported worldwide. [1]. In these individuals, muscle control is reflected in their ability to generate torque and in their difficulty regulating mechanical resistance around the joints. Consequently, rehabilitation programs can serve as an effective means for many of these individuals with disabilities to recover their physical function and reintegrate into daily life [2-3]. Throughout the continuously treatment sessions, the pre-defined exercises are assigned to individuals with disabilities which are manually provided by the physicians to evaluate the treatment process. However, this approach is expensive, as it demands continuous involvement of medical professionals and specialists to monitor each patient's movements [4-5]. The

combination of wearable robotic technologies, including an elbow exoskeleton system, and sophisticated control technologies is playing the role of facilitating the production of new tools and approaches to improve the therapeutic results. Wearable exoskeletons improve human performance, aiding human motions to minimize the user's effort, and decreasing fatigue [6]. Exoskeleton systems are patient-centric sports equipment's, as well as end-effector systems, which offer in-depth control of the joint angle and torque, thus making them an appropriate robotic modality in rehabilitative interventions in patients with severe motor issues due to brain injury. To perform its work, these exoskeleton technologies have flexible by mechanical components that rely on actuators and sensor technology to perform their duties appropriately. [7].

To provide better functionality of the exoskeleton system, numerous studies have been developed to examine the designing a controller for the system.

For example, Barbouch et al. were able to determine the efficacy of a feedback error learning algorithm combined with sliding-mode control (SMC) to possible movements of an elbow-joint using a validated electrical simulation environment [8]. On a similarly related Nguyen et al. [9] attempted to design an adaptive intelligent controller by integrating the fuzzy logic (FL) concept with conventional PID control, particularly on upper-limb exoskeleton robots where motor power is concentrated on pneumatic artificial muscles. PID controller compensates approximation error and hysteresis, and the FL component approximates nonlinear equations. A huge number of authors would choose the usage of swarm optimization to discover the optimal value of the setting parameters of a controller [10-12]. In a related article, [13] used the Whale Optimization Algorithm (WOA) to improve the effectiveness of SMC in the control of an elbow exoskeleton system; and, respectively, such approaches were studied by Hu et al. [14] introduced an assist-as-needed control strategy tailored for adaptive exoskeletons used in upper-limb rehabilitation for individuals with physical impairments. The elbow exoskeleton is powered by versatile, oppositional wire motors. In this work, Brahim et al. [15] described the back-stepping sliding-mode control scheme of tracking the preset path of an ETSMARSE exoskeleton robot during passive therapy. The robotic device is utilized by individuals with reduced upper limb capabilities because of strokes. Liu et al. [16] developed an adaptable fuzzy neural network (AFNN) to estimate elbow joint angles using sEMG. The AFNN outperformed alternative neural network concepts, including back-propagation and radial basis NN, in terms of speed and precision. Yang et al. [17] introduced a model-free back-stepping sliding-mode based control method. A non-singular quick output-sliding controller is used with an external back-stepping controller to enhance the efficacy of control. The aggregated uncertainties have been determined via time delay prediction. In the same way, Waheed et al. [18] optimized the back-stepping sliding mode control using particle swarm optimization for elbow joint angles. Bembli et al. [19] developed an adaptive sliding mode approach that relies on gravitational correction for handling upper limb exoskeleton systems with parameter constraints. This rehabilitation approach uses a robotic system with two degrees of freedom to assist in controlling elbow and shoulder movements. In this study, Islam et al. [20] have suggested a fractional sliding mode control (FSMC) method to control a 7-DOF upper-limb exoskeleton, even without the consideration of accurate kinematic modeling. FSMC outperformed SMC with regard to of control signal monitoring and chattering.

Building on insights from previous studies and aiming to explore alternative control strategies.

The current research paper comes up with a solution plan of trajectory-following an elbow exoskeleton based on the sliding mode control (SMC) approach as follows.

Chattering (i.e. high-frequency oscillations in control and state variables) is undesirable phenomenon that occurs in the classical SMC because it degrades system performance. To reduce the chattering phenomenon in the SMC, power rate (SMC_PR) and boundary layer (SMC_BL) reaching laws are introduced. The design variables of SMC affect its effectiveness. Traditionally, the determination for these variables is established by trial and error. However, integration modern optimization techniques are necessary to find these variables to improve the effectiveness of SMC. In this context, a heap-based algorithm (HBA) is used to narrow the mentioned design parameters of the SMC_PR and the SMC_BL.

2. Mathematical Model

The exoskeleton is shown in Figure 1, on the elbow joint. The device applies an actuator, which is used to help the patients in doing joint motions as indicated in [13].

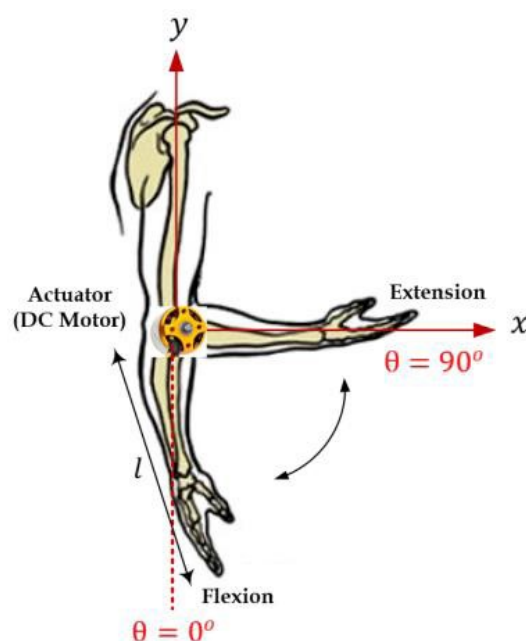


Figure 1: provides a visual overview of the elbow's flexion and extension movements

The biological arm and the exoskeleton dynamic models are developed in different ways. Then, the Euler-Lagrange equation is applied in accordance with the approach presented in [21-22].

$$L = E_k - E_g \quad (1)$$

$$\frac{d}{dt} \frac{\partial L}{\partial \dot{\theta}} - \frac{\partial L}{\partial \theta} = \tau \quad (2)$$

The system's kinetic and gravitational energy, E_k and E_g , are expressed by the following equation as follows:

$$E_k = \frac{1}{2} I \dot{\theta}^2 \quad (3)$$

$$E_g = gml(1 - \cos \theta) \quad (4)$$

Anywhere in this expression, I signify the moment of inertia of the human elbow, and m , g , and l signify the mass, the acceleration of gravity, and the distance between the elbow joint and the centre of gravity respectively, according to [13].

$$I = \frac{1}{2} ml^2 \quad (5)$$

This step can be achieved by replacing Eq. (3) and Eq. (4) in Eq. (1) to get the following result,

$$L = \frac{1}{2} I \dot{\theta}^2 - gml(1 - \cos \theta) \quad (6)$$

$$\tau_e = \tau_k + \tau_i \quad (7)$$

$$\tau_g = gml \quad (8)$$

In the last two equations, the characteristics of the torque τ_g and τ_e mean gravitational and external of the system, the torque τ_k and τ_i are called the frictional and motor control torque respectively.

$$\tau_k = K_v \dot{\theta} \quad (9)$$

Here, K_v represents the viscous friction coefficient. By applying the Euler-Lagrange equation to derive Equation (6), the system's dynamic behaviour is illustrated as shown below [18]:

$$\tau_i = I \ddot{\theta} + \tau_g \sin \theta \quad (10)$$

Substitute Eq. (9) and (10) into (7) gives:

$$\tau_e = K_v \dot{\theta} + I \ddot{\theta} + \tau_g \sin \theta \quad (11)$$

Additionally, Eq. (11) can be expressed using state variables as follows:

$$\dot{x}_1 = \dot{\theta} = x_2 \quad (12)$$

$$\dot{x}_2 = \ddot{\theta} = \frac{1}{I} (\tau_e - K_v x_2 - \tau_g \sin(x_1)) \quad (13)$$

For the purpose of controlling design, Eq. (16) can be rewritten as follows:

$$\dot{x}_2 = f(X) + bu \quad (14)$$

where:

$$f(X) = \frac{1}{I} (-K_v x_2 - \tau_g \sin(x_1))$$

$$b = \frac{1}{I}$$

3. Sliding Mode Control Design

Sliding mode control (SMC) is a recognized durable and methodical designing controller. It has two phases. The first phase is to define the surfaces that slide such that they meet the performance requirements. The next phase involves maintaining the system on the sliding surface. [23-26].

Define the tracking error as:

$$e = x_d - x_1 \quad (15)$$

where x_1 is angular position output and x_d is the desired angular position. Taking the first derivative of e yields:

$$\dot{e} = \dot{x}_d - \dot{x}_1 = \dot{x}_d - x_2 \quad (16)$$

Taking the second derivative of e yields:

$$\ddot{e} = \ddot{x}_d - \dot{x}_2 \quad (17)$$

Substitute \dot{x}_2 from Eq. (14) into Eq. (17) obtains:

$$\ddot{e} = \ddot{x}_d - f(X) - bu \quad (18)$$

The formalism of the sliding surface is the following:

$$s = \dot{e} + a_{smc} e \quad (19)$$

where $a_{smc} > 0$ is one of the tuning parameters.

The application of the first derivation of the sliding surface leads to:

$$\dot{s} = \ddot{x}_d - f(X) - bu + a_{smc} \dot{e} \quad (20)$$

The second part of the SMC control law deals with switching control, which appears as a discontinuous element that drives the system to slide along a predefined surface [27-29]. For the system to stay on this surface, the derivative of the sliding surface must match the switching control. Therefore, selecting an appropriate switching control is crucial to minimize the chattering effect commonly associated with SMC. In this study, two reaching laws are proposed to address this issue. The main component, which is known as the power rate (PR) reaching law, is used in the switching control and has been postulated in references [3031]:

$$\dot{s} = -k_{PR} |s|^p \text{sgn}(s) \quad (21)$$

The tuning parameter, which is a strictly positive number, is denoted as k_{PR} with real-valued tuning parameters denoted by ρ , whose value must remain within the bounds of 0 and 1 according to the sign function and is represented as:

$$\text{sgn}(s) = \begin{cases} +1 & \text{if } s > 0 \\ -1 & \text{if } s < 0 \end{cases} \quad (22)$$

PR reaching law eliminates the chattering because the control signal changes gradually. The last u_{PR} is obtained by putting in Eq. (21) is equal to Eq. (21) which according to them is as follows:

$$\ddot{x}_d - f(X) - bu_{PR} + a_{PR}\dot{e} = -k_{PR}|s|^\rho \text{sgn}(s) \quad (23)$$

Rearrange Eq. (23) to find u_{PR} :

$$u_{PR} = \left(\frac{1}{b}\right) (\ddot{x}_d - f(X) + a_{PR}\dot{e} + k_{PR}|s|^\rho \text{sgn}(s)) \quad (24)$$

The second reaching law is the boundary layer (BL) reaching law which is given by [32-33]:

$$\dot{s} = -k_{BL} \text{sat}(s/\phi) \quad (25)$$

where k_{PR} is adjusted parameter > 0 , $\text{sat}(s/\phi)$ is given by:

$$\text{sat}\left(\frac{s}{\phi}\right) = \begin{cases} +1 & \text{if } \frac{s}{\phi} > 0 \\ \frac{s}{\phi} & \text{if } -1 < \frac{s}{\phi} < 1 \\ -1 & \text{if } \frac{s}{\phi} < -1 \end{cases} \quad (26)$$

The last u_{BL} is given by putting Eq. (25) and is equal to Eq. (20) as given:

$$\ddot{x}_d - f(X) - bu_{BL} + a_{BL}\dot{e} = -k_{BL} \text{sat}(s/\phi) \quad (27)$$

Rearrange Eq. (27) to find u_{BL} :

$$u_{BL} = \left(\frac{1}{b}\right) (\ddot{x}_d - f(X) + a_{BL}\dot{e} + k_{BL} \text{sat}\left(\frac{s}{\phi}\right)) \quad (28)$$

4. Heap-based Algorithm

Meta-heuristic algorithms have become crucial sportive-tools for addressing a wide range of complex engineering problems [34]-[36]. In contrast to traditional trial-and-error approaches, recent studies commonly treat the tuning of controller design parameters as an optimization problem,

which is then tackled using appropriate optimization methods [37]-[40]. The work by Qamar et al. [41] introduced such a new optimization method as the heap based optimizer (HBO), which is based on the employee needs and roles. The method takes into account the corporate rank hierarchy (CRH), a common structure used in most organizations. In it, a collection of strategies is employed to partition the jobs into distinct responsibilities [42]. The HBO is built on as follows:

A heap data structure is used for describing the company level structure, the corporate hierarchy (CHR) in HBO, brings out the population as a whole. The top node in the heap corresponds to the fitness of a search agent, while each node's cost is determined by its position within the population. In this hierarchical setup, those at the highest level set the rules and restrictions, and the lower levels (children) follow the guidance of their direct supervisors (parent nodes). To imitate this type of behavior, each agent that searches \vec{h}_i location is modified by considering its parent node B , as shown in Eq. (29).

$$h_i^k(t+1) = B^k + \gamma \lambda^k |B^k - h_i^k(t)| \quad (29)$$

The current iteration index is represented by a value, t , whereas the k -th value of a particular vector is denoted by the index, k . The transformations are denoted by the parameter λ^k is element of the vector $\vec{\lambda}$, in the case of the multiplier where a stochastic parameter r is generated as follows:

$$\vec{\lambda} = 2r - 1 \quad (30)$$

Additionally, the parameter γ given in Eq. (29) is determined by the following method:

$$\gamma = \left| 2 - \frac{(t \bmod \frac{T}{c})}{\frac{T}{c}} \right| \quad (31)$$

Here, c and T are the value that is to be prescribed and the largest forfeitable number of iterations respectively. The auxiliary amount, which is denoted by the symbol γ , decreases linearly between 2 to 0 and then increases slowly until it reaches the amount 2.

In the next step, as the communication amongst co-workers, HBO workers have the similar level and rank as their co-workers. \vec{h}_i is adjusted with respect to its random partner \vec{S}_r via Eq. (32) [43].

$$h_i^k(t+1) = \begin{cases} S_r^k + \gamma \lambda^k |S_r^k - h_i^k(t)|, f(\vec{S}_r) < f(\vec{h}_i(t)) \\ h_i^k + \gamma \lambda^k |S_r^k - h_i^k(t)|, f(\vec{S}_r) \geq f(\vec{h}_i(t)) \end{cases} \quad (32)$$

The primary goal of the function (f) calculates the search agent's fitness. If $f(\vec{S}_r) < f(\vec{h}_i(t))$, Eq. (32) allows the searching agents to investigate the area around \vec{S}_r^k , otherwise, around \vec{h}_i^k . In the subsequent generation, self-contribution involves storing the prior worker status in the following order:

$$h_i^k(t+1) = h_i^k(t) \quad (33)$$

A roulette wheel is used in order to regulate both exploration as well as extraction. The population is divided into three different proportions, which are denoted as (p_1, p_2, p_3) , where p_1 gives search agents

$$h_i^k(t+1) = \begin{cases} h_i^k(t), & p \leq p_1 \\ B^k + \gamma^{\lambda^k} |B^k - h_i^k(t)|, & p > p_1 \text{ and } p \leq p_2 \\ S_r^k + \gamma^{\lambda^k} |S_r^k - h_i^k(t)|, & p > p_2 \text{ and } p \leq p_3 \text{ and } f(\vec{S}_r) < f(\vec{h}_i(t)) \\ h_i^k + \gamma^{\lambda^k} |S_r^k - h_i^k(t)|, & p > p_2 \text{ and } p \leq p_3 \text{ and } f(\vec{S}_r) \geq f(\vec{h}_i(t)) \end{cases} \quad (37)$$

where, p in $[0, 1]$ is an arbitrary number. Eq. (33) improve investigation, Eq. (29) improve exploitation and integration whereas Eq. (32) improves both.

5. Results of Numerical Simulations

The numerical simulation was coded using MATLAB program. Table 1 indicates the values of the physical parameters in the elbow exoskeleton system. The cost function used by the HBA namely the integral of absolute error (IAE) was identified to achieve optimal performance of SMC_PR and SMC_BL. This IAE is expressed as [44]:

$$IAE = \int_0^{t_{sim}} |e| dt \quad (38)$$

where t_{sim} signifies the simulation duration, and e is the output deviation, which represents the difference between the angular position of wearable exoskeleton and the required angular position. Table 2 shows the values for the planned parameters SMC_PR and SMC_BL.

Table 1. Model physical specifications

Parameters	Value
Length (l)	0.24 m
Mass (M)	1.55 kg
gravity acceleration(g)	9.81 m/s ²
Viscous friction coefficient (kv)	1.5 Nm/(rad/s)

Table 2. Optimal value of configuration parameters

Controller	Parameters	Values
SMC_PR	a_{PR}	42.4
	k_{PR}	147.8
	P	0.8
SMC_BL	a_{BL}	31.4
	k_{BL}	162.7
	ϕ	0.2

a chance to update their positions.

Values of p_1 , p_2 , and p_3 are calculated as described in Eq. (22)-(24) In which T is the repeated iteration and also the maximum number of permissible iterations.

$$p_1 = 1 - \frac{t}{T} \quad (34)$$

$$p_2 = p_1 + \frac{1 - p_1}{2} \quad (35)$$

$$p_3 = p_2 + \frac{1 - p_1}{2} = 1 \quad (36)$$

To summarize, the technique for adjusting the search agent locations is listed below:

5.1. Normal Operation

This simulation is to evaluate the performance of the two controllers in normal operation. Figure 2 and Figure 3 show the response and the control laws for the two controlled systems, correspondingly. Table 3 shows the equivalent numerical values for t_s and IAE.

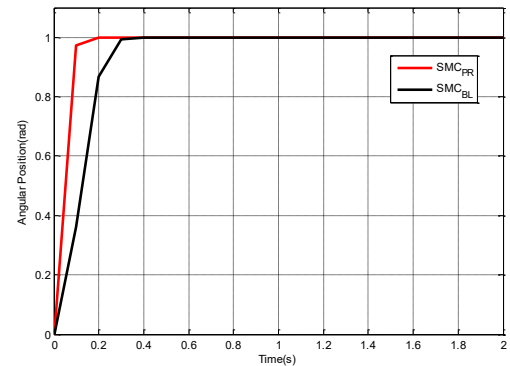


Figure 2: System response of SMC_PR and SMC_BL under normal operation

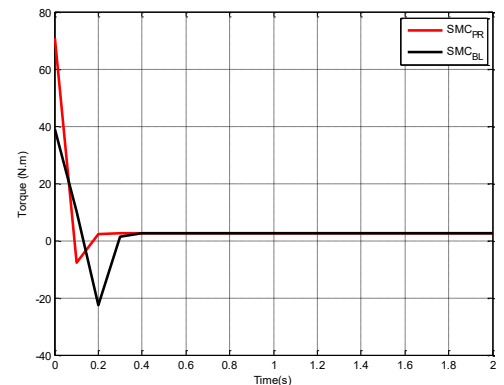


Figure 3: Control law of SMC_PR and SMC_BL under normal operation

Table 3. Comparison of dynamic performance under normal operation

Performance	SMC_PR	SMC_BL
t_s (s)	0.12	0.28
IAE (rad)	1.02	1.78

Figure 2 shows that the SMC_PR outperforms the SMC_BL. This finding may be corroborated mathematically using Table 3, which clearly shows that the value of t_s (0.12) and IAE (1.02) for SMC_PR is less than the value t_s (0.28) and IAE (1.78) for SMC_BL.

5.2. Uncertainty

To assess the durability of the two controllers against uncertainty, it was anticipated that the viscous friction coefficient (k_v) would fluctuate by 20% of its value. Figures 4 and 5 depict the response and control laws of the two controlled systems when k_v is altered by 20%, correspondingly. Table 4 contains the related numerical values of the settling time t_s and the IAE.

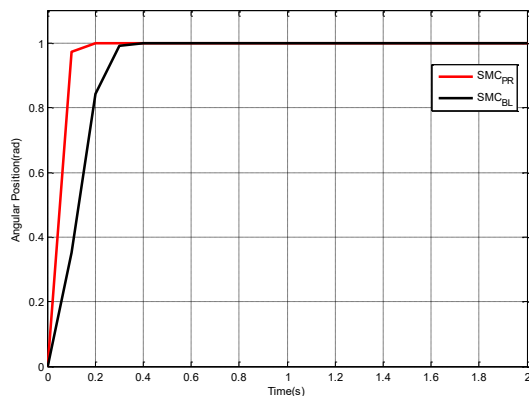


Figure 4: System response of SMC_PR and SMC_BL under uncertainty

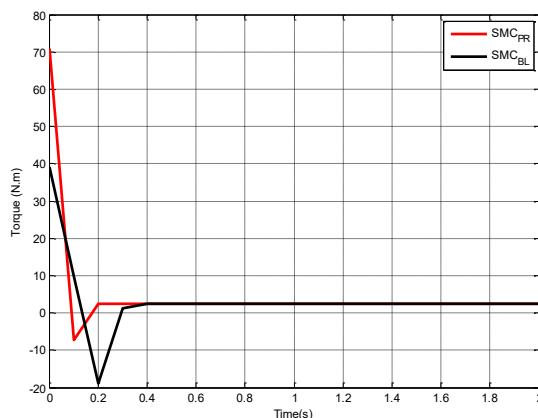


Figure 5: Control law of SMC_PR and SMC_BL under uncertainty

Table 4. Comparison of dynamic performance under uncertainty

Performance	SMC_PR	SMC_BL
t_s (s)	0.12	0.295
IAE (rad)	1.02	1.82

Table 4 illustrates that the value of t_s and IAE for the SMC_PR is not change when the value of k_v is changed by 20%. However, that the value of t_s and IAE for the SMC_BL is change when the value of k_v is changed by 20%. t_s is increased from 0.28s for the normal operation case to 0.295s when the value of k_v is changed by 20%. Moreover, IAE is increased from 1.78rad for the normal operation case to 1.82 rad when the value of k_v is changed by 20%. These results reveal that SMC_PR has more robustness characteristic than SMC_BL. Some limitations have been identified in this study; in particular, the input constraints were not considered and can be explored in future research.

6. Conclusions

The practice of using appropriate exoskeleton has emerged as an important tendency to help patients with muscle weakness to live their lives by using an appropriate system. In this paper, the wearable elbow exoskeleton system based on sliding mode control (SMC) has been developed. To obtain the mathematical model of the system, the Euler-Lagrange formulation was used. Based on the selected reaching law method, two SMC schemes are designed. In the first approach, the SMC based power rate (SMC_PR) reaching law is used, whereas in the second approach, the SMC based boundary layer (SMC_BL) reaching law is adopted. The performance of the controllers was enhanced by employing the heap-based algorithm (HBA) to tune design parameters. The numerical results have showed that both control schemes addressed the chattering problem in the output response and the control signal. Moreover, the SMC_PR performs better than the traditional SMC in the aspects of system speed, tracking error and resilience to type of parameters change.

References

- [1] J. Miguel-Fernández, J. Lobo-Prat, E. Prinsen, J. Font-Llagunes, and L. Marchal-Crespo, "Control strategies used in lower limb exoskeletons for gait rehabilitation after brain injury: a systematic review and analysis of clinical effectiveness," *Journal of neuroengineering and rehabilitation*, vol. 20, no. 1, p.23, 2023.

- [2] F.J. Badesa, R. Morales, N. Garcia-Aracil, J.M. Sabater, A. Casals, and L. Zollo, "Auto-adaptive robot-aided therapy using machine learning techniques," *Computer methods and programs in biomedicine*, vol. 116, no. 2, pp.123-130, 2014.
- [3] M.R. Islam, M. Assad-Uz-Zaman, B. Brahmi, Y. Bouteraa, I. Wang, and M.H. Rahman, "Design and development of an upper limb rehabilitative robot with dual functionality," *Micromachines*, vol. 12, no. 8, p.870, 2021.
- [4] S.M. Mahdi, N.Q. Yousif, A.A. Oglah, M.E. Sadiq, A.J. Humaidi, and A.T. Azar, A.T., "Adaptive synergetic motion control for wearable knee-assistive system: a rehabilitation of disabled patients," *Actuators*, vol. 11, no. 7, pp. 176, 2022.
- [5] A. Zahedi, Y. Wang, U. Martinez-Hernandez, and D. Zhang, "A wearable elbow exoskeleton for tremor suppression equipped with rotational semi-active actuator," *Mechanical Systems and Signal Processing*, vol. 157, p.107674, 2021.
- [6] A. Nasr, S. Bell, and J. McPhee, "Optimal design of active-passive shoulder exoskeletons: A computational modeling of human-robot interaction," *Multibody System Dynamics*, vol. 57, no. 1, pp.73-106, 2023.
- [7] H. Herr, "Exoskeletons and orthoses: classification, design challenges and future directions," *Journal of NeuroEngineering and Rehabilitation*, vol. 6, no. 21, pp. 1-9, 2009.
- [8] H. Barbouch, F. Resquin, J. Gonzalez-Vargas, N.K. Haddad, S. Belghith, "Feedback error learning with sliding mode control for functional electrical stimulation elbow joint simulation," *International Journal of Innovative Technology and Exploring Engineering (IJITEE)*, vol. 8, issue. 12, pp. 2971-2982, Oct. 2019. doi.org/10.35940/ijitee.K2026.1081219
- [9] H.T. Nguyen, V.C. Trinh, T.D. Le, (2020), "An adaptive fast terminal sliding mode controller of exercise-assisted robotic arm for elbow joint rehabilitation featuring pneumatic artificial muscle actuator", *Actuators*, vol. 9, issue. 4, pp. 118, Nov. 2020. doi.org/10.3390/act9040118
- [10] M.A. Al-Ali, O.F. Lutfy and H. Al-Khazraj, "Investigation of optimal controllers on dynamics performance of nonlinear active suspension systems with actuator saturation," *Journal of Robotics and Control (JRC)*, vol. 5, no. 4, pp.1041-1049, 2024.
- [11] G.W. Abedulabbas, and F.R. Yaseen, "Sensorless Speed Control of a Brushless DC Motor Using Particle Filter (PF)," *Mathematical Modelling of Engineering Problems*, vol. 9, no. 6, pp. 1523-1531, 2022.
- [12] F.R. Al-Ani, O.F. Lutfy and H. Al-Khazraj, "Optimal Synergetic and Feedback Linearization Controllers Design for Magnetic Levitation Systems: A Comparative Study," *Journal of Robotics and Control (JRC)*, vol. 6, no. 1, pp.22-30, 2025.
- [13] Z.A. Waheed, and A.J. Humaidi, "Design of optimal sliding mode control of elbow wearable exoskeleton system based on whale optimization algorithm," *Journal Européen des Systèmes Automatisés*, vol. 55, no. 4, p.459, 2022.
- [14] B. Hu, F. Zhang, H. Lu, H. Zou, J. Yang, H. Yu, "Design and assist-as-needed control of flexible elbow exoskeleton actuated by nonlinear series elastic cable driven mechanism", *Actuators*, vol. 10, issue. 11, pp. 290, Oct. 2021. doi.org/10.3390/act10110290
- [15] B. Brahmi, M. Rahman, M. Saad, C.O. Luna, M.R. Islam, "Sliding mode-backstepping control for upper-limb rehabilitation with the ets-marse exoskeleton robot", *RESNA: Arlington, VA, USA*, pp. 1-7, Jun. 2016.
- [16] Y. Liu, C. Li, Z. Teng, K. Liu, G. Wang, Z. Sun, "Intention recognition of elbow joint based on sEMG using adaptive fuzzy neural network", In 2020 5th International Conference on Mechanical, Control and Computer Engineering (ICMCCE), Harbin, China, pp. 1091-1096, Dec. 2020. doi.org/10.1109/ICMCCE51767.2020.00240
- [17] P. Yang, J. Sun, J. Wang, G. Zhang, Y. Zhang, "Model-free based back-stepping sliding mode control for wearable exoskeletons", In 2019 25th International Conference on Automation and Computing (ICAC), pp.1-6, Sep. 2019. doi.org/10.23919/ICAC.2019.8895069
- [18] Z.A. Waheed, A.J. Humaidi, M.E. Sadiq, A.A. Al-Qassar, A.F. Hasan, A.Q. Al-Dujaili, A.R. Ajel, and S.J. Abbas, "Control of elbow rehabilitation system based on optimal-tuned backstepping sliding mode controller," *J. Eng. Sci. Technol*, vol. 18, no. 1, pp.584-603, 2023.
- [19] S. Bembli, N.K. Haddad, S. Belghith, "Adaptive sliding mode control with gravity compensation: Application to an upper-limb exoskeleton system", In *MATEC Web of Conferences*, vol. 261, pp. 06001, Jan. 2019. doi.org/10.1051/mateconf/201926106001
- [20] M.R. Islam, M. Rahmani, M.H. Rahman, "A novel exoskeleton with fractional sliding mode control for upper limb rehabilitation", *Robotica*, vol. 38, issue. 11, pp. 2099- 2120, Jan. 2020. doi.org/10.1017/S0263574719001851
- [21] R. A. Kadhimi, M. Q. Kadhimi, H. Al-Khazraji, and A. J. Humaidi, "Bee algorithm based control design for two-links robot arm systems," *IJUM Engineering Journal*, vol. 25, no. 2, pp. 367-380, 2024.
- [22] K. Al-Badri, H. Dulaimi, H. Al-Khazraji, and A.J. Humaidi, "Adaptive Neural Network Control for Load-Varying Two-Link Robots Using Honey Badger Optimization," *Journal of Robotics and Control (JRC)*, vol. 6, no. 2, pp.1061-1068, 2025.

- [23] F. Haroon, M. Aamir, A. Waqar, S. Mian Qaisar, S.U. Ali, and A.T. Almaktoom, "A composite exponential reaching law based SMC with rotating sliding surface selection mechanism for two level three phase VSI in vehicle to load applications," *Energies*, vol. 16, no. 1, p.346, 2022.
- [24] B. Nawress, A.N. Gharbi, and N.B. Braiek, "Sliding Mode Control based on Neural State and Disturbance Observers: Application to a Unicycle Robot Using ROS2," *Journal of Robotics and Control (JRC)*, vol. 5, no. 4, pp.964-980, 2024.
- [25] A. Hassan, M. Nawfal, H. Al-Khazraji, and A. Humaidi, "Improved of Sliding Mode Control for Maximum Power Point Tracking in Solar Photovoltaic Applications Under Varying Conditions," *International Journal of Robotics and Control Systems*, vol. , no. 3, pp. 1790-1807, 2025.
doi:<https://doi.org/10.31763/ijrcs.v5i3.1925>
- [26] K. Adamiak, and A. Bartoszewicz, "Novel power-rate reaching law for quasi-sliding mode control," *Energies*, vol. 15, no. 15, p.5446, 2022.
- [27] A. Ma'arif, M. Antonio, M., Sadek, E. Umoh and A. Abougarair, R. Nurindra, "Sliding Mode Control Design for Magnetic Levitation System," *Journal of Robotics and Control (JRC)*, vol. 3, no.6, pp. 848-853, 2022.
- [28] H. Al-Khazraji, K. Al-Badri, R. Al-Majeez, and A.J. Humaidi, "Synergetic control design based sparrow search optimization for tracking control of driven-pendulum system," *Journal of Robotics and Control (JRC)*, vol. 5, no. 5, pp.1549-1556, 2024.
- [29] N. Qiao, L. Wang, M. Liu, and Z. Wang, "The sliding mode controller with improved reaching law for harvesting robots," *Journal of Intelligent & Robotic Systems*, vol. 104, no. 1, p.9, 2022.
- [30] H. Al-Khazraji, R.M. Naji, and M.K. Khashan, "Optimization of sliding mode and back-stepping controllers for AMB systems using gorilla troops algorithm," *Journal Européen des Systèmes Automatisés*, vol. 57, no. 2, p.417, 2024.
- [31] P. Latosiński, "Sliding mode control based on the reaching law approach—A brief survey," In 2017 22nd International conference on methods and models in automation and robotics (MMAR), 2017, pp. 519-524).
- [32] W. Gao, and J.C. Hung, J.C., "Variable structure control of nonlinear systems: A new approach," *IEEE transactions on Industrial Electronics*, vol. 40, no. 1, pp.45-55, 1993.
- [33] A.M. Hameed, and A.K. Hamoudi, "A 2-link robot with adaptive sliding mode controlled by barrier function," *Journal Européen des Systèmes Automatisés*, vol. 56, no. 6, p.1105, 2023.
- [34] A. K. Hamoudi, "Design and simulation of sliding mode fuzzy controller for nonlinear system," *Journal of Engineering*, vol. 22, no. 3, pp.66-76, 2016.
- [35] S. Khlil, H. Al-Khazraji and Z. Alabacy, "Solving assembly production line balancing problem using greedy heuristic method," In *IOP Conference Series: Materials Science and Engineering*, vol. 745, no. 1, p. 012068, 2020.
- [36] H. Al-Khazraji, S. Khlil and Z. Alabacy, "Industrial picking and packing problem: Logistic management for products expedition", *Journal of Mechanical Engineering Research and Developments*, vol.43, no.2, pp.74-80, 2020.
- [37] H. Al-Khazraji, A.R. Nasser and S. Khlil, "An intelligent demand forecasting model using a hybrid of metaheuristic optimization and deep learning algorithm for predicting concrete block production", *IAES International Journal of Artificial Intelligence*, vol.11, no.2, p.649-657, 2022.
- [38] F.R. Yaseen, M.Q. Kadhim, H. Al-Khazraji and A.J. Humaidi, "Decentralized Control Design for Heating System in Multi-Zone Buildings Based on Whale Optimization Algorithm," *Journal Européen des Systèmes Automatisés*, vol. 57, no. 4, pp. 981-989, 2024.
- [39] H. Al-Khazraji, K. Albadri, R. Almajeez and A.J. Humaidi, "Synergetic Control-Based Sea Lion Optimization Approach for Position Tracking Control of Ball and Beam System," *International Journal of Robotics and Control Systems*, vol. 4, no.4, pp.1547-1560, 2024.
- [40] N. M. Alyazidi, A. M. Hassanine, M. S. Mahmoud and A. Ma'arif, "Enhanced Trajectory Tracking of 3D Overhead Crane Using Adaptive Sliding-Mode Control and Particle Swarm Optimization", *Journal of Robotics and Control (JRC)*, vol. 5, no. 1, pp.253-262, 2024.
- [41] H. Al-Khazraji, W. Guo and A.J. Humaidi, "Improved Cuckoo Search Optimization for Production Inventory Control Systems", *Serbian Journal Of Electrical Engineering*, vol.21, no.2, pp.187-200, 2024.
- [42] Q. Askari, M. Saeed, and I. Younas, "Heap-based optimizer inspired by corporate rank hierarchy for global optimization," *Expert Systems with Applications*, vol. 161, p.113702, 2020.
- [43] D.S. Abdelminaam, E.H. Houssein, M. Said, D. Oliva, and A. Nabil, "An efficient heap-based optimizer for parameters identification of modified photovoltaic models," *Ain Shams Engineering Journal*, vol. 13, no. 5, p.101728, 2022.
- [44] A.K. Ahmed, H. Al-Khazraji, and S.M. Raafat, "Optimized PI-PD Control for Varying Time Delay Systems Based on Modified Smith Predictor," *International Journal of Intelligent Engineering & Systems*, vol. 17, no. 1, pp. 331-342, 2024.
- [45] H. Al-Khazraji, C. Cole, and W. Guo, "Dynamics analysis of a production-inventory control system with two pipelines feedback," *Kybernetes*, vol. 46, no. 10, pp.1632-1653, 2017.